*fishes*

MDPI

*Article*

# Genetic Diversity and Population Structure Analysis of Chinese Mitten Crab (*Eriocheir sinensis*) in the Yangtze and Liaohe Rivers

**Lin Zhou [1], Jiancao Gao [2], Yanping Yang [2], Zhijuan Nie [2], Kai Liu [2] and Gangchun Xu [1,2,*]**

[1] College of Fisheries and Life Science, Shanghai Ocean University, Shanghai 201306, China
[2] Freshwater Fisheries Research Center, Chinese Academy of Fishery Sciences, Wuxi 214081, China
* Correspondence: xugc@ffrc.cn; Tel.: +86-0510-8539-0029

**Abstract:** Recently, the economic traits of Chinese mitten crab (*Eriocheir sinensis*) varieties have had a negative tendency. Meanwhile, the status of wild germplasm resources of *E. sinensis* is unknown, hindering the utilization of wild germplasm resources and the green development of the *E. sinensis* industry. Thus, the conservation of the wild *E. sinensis* germplasm resource is of great significance. To this end, we collected wild *E. sinensis* from two different river basins, the Yangtze River basin, and the Liaohe River basin, and analyzed the genetic diversity as well as the genetic differentiation in *E. sinensis* populations. Based on eight microsatellite markers, we found moderate genetic diversity in *E. sinensis* populations regardless of river basin. Based on the mitochondrial D-loop region, we found that all populations are at mutation drift equilibrium, while the *Nm* between any two populations is greater than 1. We hypothesized the existence of island model gene flow patterns among *E. sinensis*. Interestingly, genetic differentiation among *E. sinensis* populations was low, except that between Liaohe and Anqing or Shanghai populations. Additionally, geometric morphological analysis could distinguish *E. sinensis* from different basins, with an accuracy of 94.2–100%. Given the similar genetic diversity in the two basins, the genetic convergence of *E. sinensis* from different basins deserves further attention.

**Keywords:** crabs; D-loop sequences; microsatellite; genetic; geometric morphometrics

**Key Contribution:** The present state of wild *Eriocheir sinensis* resources in the Yangtze River and Liaohe River basins was revealed.

check for updates

**Citation:** Zhou, L.; Gao, J.; Yang, Y.; Nie, Z.; Liu, K.; Xu, G. Genetic Diversity and Population Structure Analysis of Chinese Mitten Crab (*Eriocheir sinensis*) in the Yangtze and Liaohe Rivers. *Fishes* **2023**, *8*, 253. https://doi.org/10.3390/fishes8050253

Academic Editor: Hyun-Woo Kim

Received: 13 February 2023
Revised: 22 April 2023
Accepted: 8 May 2023
Published: 10 May 2023



## 1. Introduction

Chinese mitten crab (*Eriocheir sinensis*) is an important economic aquatic animal in China. Due to the suitable environment of the middle and lower reaches of the Yangtze River basin, it has become the optimal area for *E. sinensis* growth and development [1]. The Yangtze River is the third largest river in the world, and its species diversity is ecologically vital. Previous studies have shown that Chinese mitten crabs in different basins of the Yangtze River have different genetic diversities. For example, the genetic diversity of *E. sinensis* (adult and juvenile) in the Zhenjiang region is lower than that in other regions [2]. In the 1980s, the expansion of the aquaculture scale led to a reduction in wild *E. sinensis*. Because of the shortage of wild germplasm resources, Chinese mitten crabs from other basins were introduced to the Yangtze River basin, including the Liaohe River basin [3]. In recent years, the economic shape of the cultured *E. sinensis* population has been degraded [4]. Meanwhile, the status quo of wild germplasm resources is unclear, which hinders scientific development and utilization, and is not conducive to the green development of the crab industry. In addition, in order to improve the scale and quality of crab aquaculture, a large number of new varieties have been obtained through different selection methods [5], such as "Changjiang 1", "Changjiang 2", "Noya No. 1" and "Sea & River 21" [6]. Although new species temporarily relieve breeding needs, the wild Yangtze

crab is still a high-quality parent variety for selection and breeding [4]. Therefore, it is particularly important to investigate their population structure and availability of germplasm. In order to investigate the current state of wild *E. sinensis* germplasm resources and clarify the genetic differentiation relationship between different river systems of crab populations, in this study, four populations from the Yangtze River and one population from the Liaohe River were collected, and their population genetics were analyzed using the mitochondrial D-loop region and eight microsatellite markers.

Morphological characteristics are not only the important basis of taxonomy; also significant is the external expression of the genetic characteristics of species [7]. Morphology is the simplest and fastest method to identify species. Compared to traditional morphometry, geometric morphometrics is more suitable for obtaining the shape data of organisms, allowing the visual comparison of subtle differences between study subjects [8,9]. Through geometric morphometrics, it has been revealed that genital characteristics could be an indicator to distinguish giant Amazonian ants (*Dinoponera*) [10]. In *Apidae*, the size and shape of the forewing were of value in distinguishing the species [11]. A published study examined evidence that the species and sex of four planktivorous petrels can be distinguished by geometric morphometrics [12]. In addition, geometric morphometrics has been widely used in aquatic animals [13]. Emperor fishes (*Lethrinidae*) can be identified by geometric morphology in the late larval and early juvenile stages [14]. A previous study reported that different freshwater prawns were distinguished through chelae and carapace by geometric morphometrics [15]. In particular, it is applied to identify the geographical origin of aquatic animals, such as prawns [16], crabs [17], etc.

Morphological characteristics are determined jointly by genetic information and environment. Thus, under similar environmental conditions, morphological differences mainly contribute to genetic variations [18]. Although geometric morphometrics can accurately indicate morphological variation, it has some limitations in distinguishing populations in close geographic contact [19]. Molecular markers are specific DNA fragments that reflect some difference in the genome between individuals or populations of organisms, which is more accurate than morphology. Thereinto, microsatellite loci have the advantages of co-dominant inheritance, high polymorphism, and a large amount of information [20,21]. The D-loop region is a noncoding gene on the mitochondrial genome, located between the tRNA-Phe of mitochondrial DNA (mtDNA) [22], and it is the fastest-evolving and most abundant region in the mitochondria [23]. Microsatellites, derived from nuclear genes, are characterized by high polymorphism, sufficient quantity, rapid mutation, wide distribution, and a simple analysis methods [24,25]. Moreover, the frequency of microsatellites in the population is stable in theory, which is not subject to selection pressure [26]. Both are ideal molecular markers. The use of microsatellite analysis has been reported to confirm the finding of a single population of *Paralichthys dentatus* along the Atlantic coast [27]. Wang et al. distinguished *Gymnocypris chilianensis*, *Gymnocypris przewalskii*, and *Gymnocypris eckloni* using mitochondrial D-loop region markers and found that the latter two may be subspecies of each other [28]. A previous study successfully detected genetic differentiation in different populations of marine fishes [29]. In crustaceans, microsatellites are also widely used, often for genetic analysis [30,31]. Švara et al. conducted a microevolutionary dynamic analysis of the *Gammarus pulex* population with microsatellite markers [32]. Other authors reported that the rockpool shrimp (*Palaemon elegans*) demonstrated a weak but significant genetic differentiation between the Canary Islands and the Atlantic mainland through microsatellite analysis [33].

The current study was conducted to investigate the genetic diversity and population structure of *E. sinensis* by combining nuclear microsatellite markers, mitochondrial D-loop region sequences, and morphological methods. The aim was to estimate the diversity of the germplasm and understand the status of the germplasm resources of wild *E. sinensis* populations in the Yangtze and Liaohe river basins. The results of this study will help us understand the status of the germplasm resources and the degree of germplasm mixing of

*E. sinensis* in the two basins. It will provide valuable information on the conservation and utilization of *E. sinensis* resources.

## 2. Materials and Methods

### *2.1. Ethics Statement*

The experimental protocol was performed following the guidelines approved by the Institutional Animal Care and Use Committee of the Ministry of Freshwater Fisheries Research Center, Chinese Academy of Fishery Sciences (SYXK(HX)20210104006).

### *2.2. Sample Collection*

In total, 132 wild adults of *E. sinensis* were collected from 5 locations along the Yangtze River and Liaohe River for genetic analysis. (Figure 1). Sampling sites were located in Anqing city (AQ), Changshu city (CS), Taizhou city (TZ), Shanghai (SH), and Panjin city (LH). Sampling information of the crabs is shown in Table S1. Crab samples were photographed with a Canon EOS 70D for morphological analysis, and then muscle was collected and stored in 96% alcohol for DNA extraction.

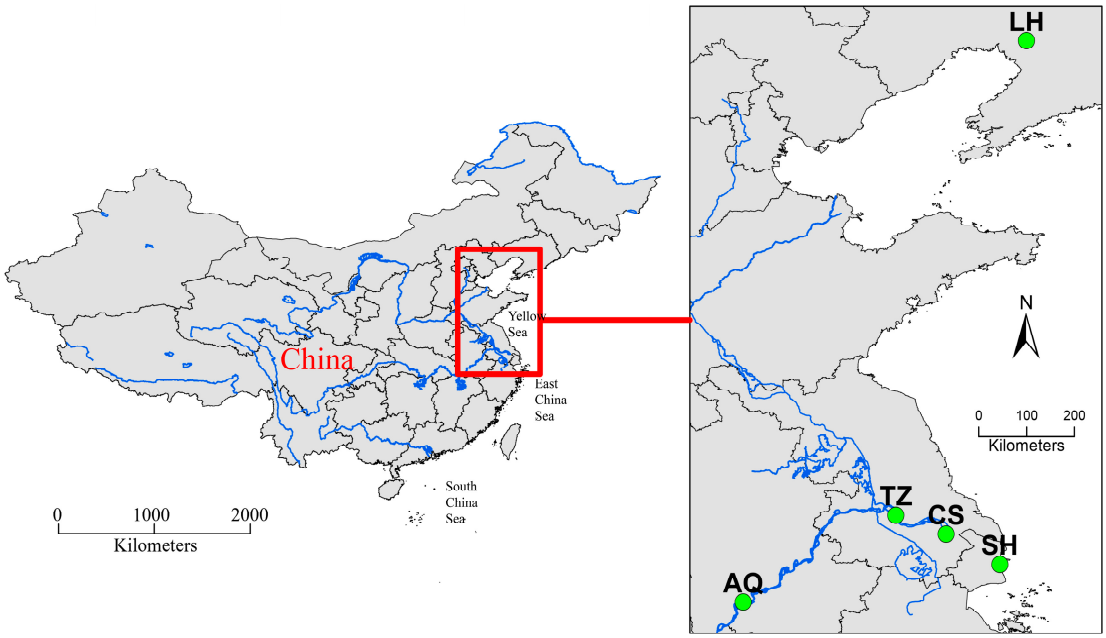


**Figure 1.** Five sampling sites in this study: Anqing city (AQ), Taizhou city (TZ), Changshu city (CS), Shanghai city (SH), and Panjin city (LH).

### *2.3. DNA Extraction, Microsatellite, and D-Loop Fragment Amplification*

DNA was extracted from muscle tissue using Universal Genomic DNA Kit (CW-BIO, Nanjing, China) according to the manufacturer's instructions. The integrity and concentration of DNA were detected by 1% agarose gel electrophoresis and Nanodrop 2000 spectrophotometer. The D-loop region sequences' amplification primers were: F: 5′-ACGTAACTGAAATGCTGTTC-3′ and R: 5′-ACCCGTTTCCCCTCTAGAGGA-3′ [34]. The PCR system of the D-loop used a 25 µL-total reaction system including 12.5 µL 2 × Taq Plus Master Mix (Vazyme, Nanjing, China), 2.5 µL DNA template, 1.25 µL each primer (10 µmol/L), and 7.5 µL sterile water. The reaction was amplified at 95 °C for 3 min, followed by 36 cycles of 95 °C for 15 s, 54 °C for 15 s, 72 °C for 30 s, and 72 °C for 5 min.

A total of eight microsatellite loci of *E. sinensis* were used to analyze the genetic variations among the five sampling populations [35]. The forward primers for each microsatellite locus were labeled with a fluorescence marker (Table S2). The PCR microsatellite system used a 10 µL-total reaction system including 5 µL 2 × Taq Plus Master Mix (Vazyme, Nanjing, China), 1 µL DNA template, 0.4 µL each primer (10 µmol/L), and 3.2 µL sterile

water. The reaction was amplified at 94 °C for 3 min, followed by 38 cycles of 94 °C for 15 s, 55 °C for 1 min, 72 °C for 1 min, and 72 °C for 5 min. Before fragment length analysis, equal amounts of PCR products were mixed into two sets (Table S2). Fragment sizes were scored manually after electrophoresis on an ABI3730 sequencer (Yixin Biotechnology, Wuxi, China), using Liz500 as the internal size standard.

### *2.4. Carapace Morphology*

In this study, 30 landmarks were used for analyzing the shape variation in carapaces (Figure S1). The tpsRelw32 was used to obtain the mean shape and the variance in each landmark. Grid deformation and variation visualization of the carapaces were calculated by MorphoJ 1.07a [36]. Discriminant analysis was conducted using SPSS 26.0 [37]. In the study, the main objective was to investigate whether the *E. sinensis* of the Yangtze and Liaohe river basins could be effectively distinguished by geometric morphology. In addition, a total of 54 *E. sinensis* carapaces from the Liaohe River basin and 172 from the Yangtze River basin were collected for analysis.

### *2.5. Molecular Genetic Analysis*

Multiple alignments of mitochondrial D-loop region sequences was conducted using Clustalx [38]. The nucleotide diversity ($P_i$) and haplotype diversity ($H_d$), were analyzed by DnaSP 5.10 [39]. The fixation index ($F_{ST}$), gene flow ($N_m$), analysis of molecular variance (AMOVA), Tajima's D, and Fu's Fs test values were determined in Arlequin 3.5 [40]. The haplotype network was implemented by the median-joining method through POPART 1.7 [20]. A neighbor-joining phylogenetic tree and maximum likelihood tree were constructed based on the Kimura 2-parameter model by MAGE 11. Bootstrap values were based on 1000 rapid bootstrap replicates.

The Micro-checker was used to detect null alleles at each locus [41]. Analysis of molecular variance (AMOVA), expected heterozygosity ($H_e$), observed heterozygosity ($H_o$), and fixation index ($F_{ST}$) were then calculated for each microsatellite marker using Arlequin 3.5 [40], as well as the Hardy–Weinberg test. Allelic richness ($A_R$) was calculated using FSTAT v 2.9.3 [42]. The Bayesian clustering analyses run in STRUCTURE v 2.3.4 were evaluated using the Evanno test to determine the most optimal number of K [43,44]. The neighbor-joining (N-J) tree was then constructed based on Nei's $D_A$ genetic distances by Phylip 3.695 [45]. In addition, principal coordinate analysis (PCoA) was performed on various populations based on pairwise Nei's genetic distances between populations using GenAlEx 6.51 [46,47].

## 3. Result

### *3.1. Geometric Morphometrics*

Based on 30 landmarks selected in the study, all *E. sinensis* from the Yangtze and Liaohe rivers were analyzed by geometric morphometrics so as to determine the mean shape (Figure S2A) and the overlapped shape (Figure S2B). Next, we found that the landmarks with the highest contributions were 19 and 20, which accounted for 62.262% of the variance (Table S3). Then, relative warps in the principal component (PC) analysis result showed that the variance contribution of the first two principal components was the largest (Table S4), which could explain the morphological variation in the carapaces (Figure S3A). The results showed that the combination of PC1 and PC2 can well distinguish between the populations of the Yangtze and Liaohe rivers (Figure S3B). Using PC1, the Yangtze and Liaohe populations could not be well distinguished, while using PC2, they could (Figure S3B). The PC2 value of the Liaohe population was lower than that of the Yangtze population (Figure S3B). Furthermore, after visualizing the difference in carapaces (variations were enlarged three times), it was found that the morphological characteristics were mainly different in the distance to the posterior lateral edge (Figure 2). Based on the analysis of PC2 (Figure S3D) and the grid diagram (Figure 2), the changing trend mainly

exists in the landmarks 21 and 22. The posterior lateral edge of the Yangtze population is narrower, while the posterior lateral edge of the Liaohe population is wider.

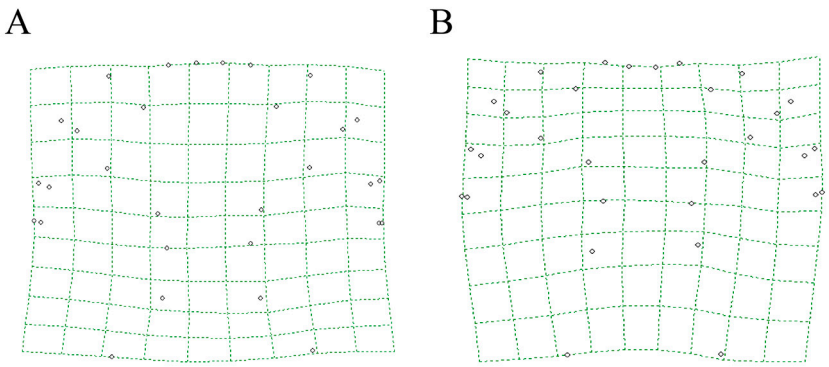


**Figure 2.** Grid deformation and variation visualization of the carapace of wild Chinese mitten crab (*E. sinensis*) (variations are enlarged three times). (**A**) Liaohe River population; (**B**) Yangtze River population. The circles represent landmarks.

Furthermore, the result of the discriminant analysis showed that the accuracy of discrimination was 94.2% and 100.0% in the Yangtze population and the Liaohe population, respectively (Table 1). The discriminant analysis showed that 56 indices were included in the discriminant function of 56 relative warp principal component scores of the carapace morphology of the two basins (the discriminatory formula is found in Supplementary Materials). Based on the discriminant function, the *E. sinensis* in the two basins could be distinguished (Figure 3).

**Table 1.** Classification results of Chinese mitten crab (*E. sinensis*) from different basins.

| Population | Liaohe River | Yangtze River |
|---|---|---|
| Liaohe River | 54 (100.0%) | 0 |
| Yangtze River | 10 (5.8%) | 162 (94.2%) |

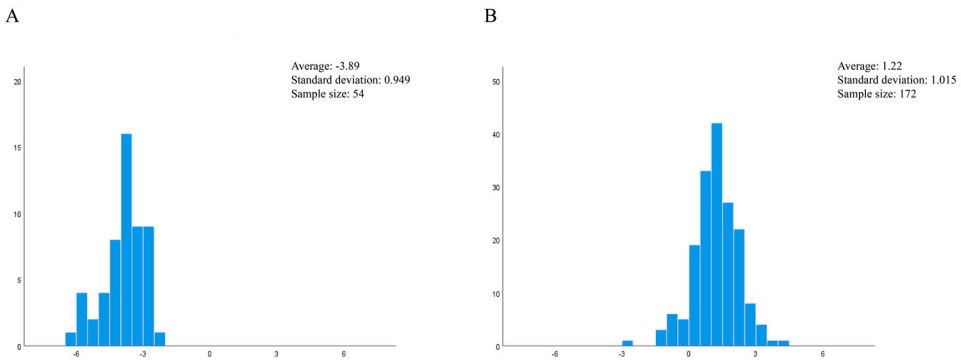


**Figure 3.** The discriminate analysis by carapace geometrical morphometry for the Chinese mitten crab (*E. sinensis*) populations. (**A**) Liaohe River population; (**B**) Yangtze River population.

### *3.2. Population Genetic Diversity*

In the present study, based on microsatellite loci data, the mean $H_o$ values ranged from 0.571 to 0.712, with the highest values observed in the SH population and the lowest in the LH population (Table 2). The mean $H_e$ values ranged from 0.653 to 0.678, with the highest values observed in the SH population (Table 2). Unlike $H_o$, the lowest mean $H_e$ values were for the AQ population rather than the LH population. The mean $A_R$ values of each microsatellite locus ranged from 5.875 to 6.530, with the highest and the lowest mean $A_R$ values observed in the Yangtze population (Table 2). Regarding the result of the

Hardy–Weinberg equilibrium, we found that some microsatellite loci in the five *E. sinensis* populations examined had an exact test probability of less than 0.05, revealing a significant deviation from the Hardy–Weinberg equilibrium (Table 3). The AQ and TZ populations had the most microsatellite loci deviating significantly from the Hardy–Weinberg equilibrium, with three loci.

**Table 2.** Observed heterozygosity ($H_o$), expected heterogeneity ($H_e$), allelic richness ($A_R$), and Hardy–Weinberg equilibrium (HWE) for 8 microsatellite loci of Chinese mitten crabs (*E. sinensis*) from the different basins.

| | Locus | CX140 | CX287 | CX256 | CX416 | CX003 | CX254 | CX400 | CX427 | Mean |
|---|---|---|---|---|---|---|---|---|---|---|
| LH | $H_o$ | 0.433 | 0.666 | 0.966 | 0.344 | 0.4 | 0.6 | 0.533 | 0.633 | 0.571 |
| | $H_e$ | 0.397 | 0.765 | 0.957 | 0.434 | 0.467 | 0.816 | 0.68 | 0.837 | 0.669 |
| | $A_R$ | 3.609 | 6.305 | 15.335 | 4.22 | 4.032 | 6.898 | 4.597 | 6.845 | 6.48 |
| | HWE | 1 | 0.246 | 0.227 | 0.185 | 0.198 | 0.001 | 0.101 | 0.023 | |
| CS | $H_o$ | 0.25 | 0.666 | 0.909 | 0.75 | 0.666 | 0.583 | 0.583 | 0.416 | 0.602 |
| | $H_e$ | 0.358 | 0.67 | 0.982 | 0.666 | 0.586 | 0.731 | 0.586 | 0.847 | 0.678 |
| | $A_R$ | 2.917 | 4.83 | 19 | 4.83 | 4 | 5.83 | 4 | 6.833 | 6.53 |
| | HWE | 0.403 | 1 | 0.138 | 0.627 | 1 | 0.34 | 0.621 | 0.001 | |
| AQ | $H_o$ | 0.533 | 0.7 | 0.966 | 0.333 | 1 | 0.633 | 0.566 | 0.566 | 0.662 |
| | $H_e$ | 0.437 | 0.788 | 0.937 | 0.375 | 0.524 | 0.769 | 0.533 | 0.866 | 0.653 |
| | $A_R$ | 3.315 | 6.376 | 13.296 | 3.69 | 2.367 | 6.536 | 4.109 | 7.727 | 5.927 |
| | HWE | 0.735 | 0.156 | 0.014 | 0.295 | 0 | 0.076 | 0.688 | 0 | |
| TZ | $H_o$ | 0.4 | 0.633 | 0.933 | 0.433 | 1 | 0.8 | 0.533 | 0.566 | 0.662 |
| | $H_e$ | 0.345 | 0.777 | 0.939 | 0.363 | 0.508 | 0.861 | 0.596 | 0.856 | 0.655 |
| | $A_R$ | 2.875 | 6.771 | 14.137 | 3.094 | 2 | 7.7 | 3.698 | 7.635 | 5.988 |
| | HWE | 1 | 0.033 | 0.827 | 0.775 | 0 | 0.485 | 0.234 | 0.001 | |
| SH | $H_o$ | 0.633 | 0.766 | 1 | 0.433 | 1 | 0.633 | 0.567 | 0.667 | 0.712 |
| | $H_e$ | 0.493 | 0.771 | 0.927 | 0.37 | 0.54 | 0.847 | 0.65 | 0.799 | 0.674 |
| | $A_R$ | 3.639 | 6.786 | 12.478 | 3.196 | 2.733 | 7.18 | 4.703 | 6.292 | 5.875 |
| | HWE | 0.537 | 0.589 | 0.239 | 1 | 0 | 0.057 | 0.223 | 0.169 | |

**Table 3.** Summary statistics for D-loop polymorphisms of five Chinese mitten crab (*E. sinensis*) populations.

| Population | Number of Haplotypes (n) | Haplotype Diversity ($H_d$) | Nucleotide Diversity ($P_i$) | Variable Sites |
|---|---|---|---|---|
| LH | 6 | 1.000 ± 0.096 | 0.02009 ± 0.00360 | 24 |
| AQ | 6 | 1.000 ± 0.096 | 0.00624 ± 0.00948 | 9 |
| CS | 4 | 1.000 ± 0.177 | 0.00948 ± 0.00225 | 9 |
| TZ | 5 | 0.933 ± 0.122 | 0.01276 ± 0.00374 | 18 |
| SH | 5 | 1.000 ± 0.126 | 0.00778 ± 0.00253 | 9 |

According to the result of the D-loop analysis, in the different populations, $H_d$ and $P_i$ values ranged from 0.933 to 1.000 and from 0.006 to 0.020 (Table 3), respectively. The TZ population showed the lowest $H_d$ value of all the populations. The LH population showed the highest $P_i$ value, and the lowest $P_i$ value was observed in the AQ population. In total, 22 haplotypes were identified, including 20 unique haplotypes, and 2 shared haplotypes: haplotype 1 in CS, AQ, and SH; and haplotype 15 in AQ, TZ, and SH (Table 4).

**Table 4.** Haplotype frequency distribution in five Chinese mitten crab (*E. sinensis*) populations from the Liaohe River and Yangtze River.

| Haplotype | CS | LH | AQ | TZ | SH | Total |
|---|---|---|---|---|---|---|
| **Hap_1** | 1 | 0 | 1 | 0 | 1 | 3 |
| Hap_2 | 1 | 0 | 0 | 0 | 0 | 1 |
| Hap_3 | 1 | 0 | 0 | 0 | 0 | 1 |
| Hap_4 | 1 | 0 | 0 | 0 | 0 | 1 |
| Hap_5 | 0 | 1 | 0 | 0 | 0 | 1 |
| Hap_6 | 0 | 1 | 0 | 0 | 0 | 1 |
| Hap_7 | 0 | 1 | 0 | 0 | 0 | 1 |
| Hap_8 | 0 | 1 | 0 | 0 | 0 | 1 |
| Hap_9 | 0 | 1 | 0 | 0 | 0 | 1 |
| Hap_10 | 0 | 1 | 0 | 0 | 0 | 1 |
| Hap_11 | 0 | 0 | 1 | 0 | 0 | 1 |
| Hap_12 | 0 | 0 | 1 | 0 | 0 | 1 |
| Hap_13 | 0 | 0 | 1 | 0 | 0 | 1 |
| Hap_14 | 0 | 0 | 1 | 0 | 0 | 1 |
| **Hap_15** | 0 | 0 | 1 | 2 | 1 | 4 |
| Hap_16 | 0 | 0 | 0 | 1 | 0 | 1 |
| Hap_17 | 0 | 0 | 0 | 1 | 0 | 1 |
| Hap_18 | 0 | 0 | 0 | 1 | 0 | 1 |
| Hap_19 | 0 | 0 | 0 | 1 | 0 | 1 |
| Hap_20 | 0 | 0 | 0 | 0 | 1 | 1 |
| Hap_21 | 0 | 0 | 0 | 0 | 1 | 1 |
| Hap_22 | 0 | 0 | 0 | 0 | 1 | 1 |

Note: Bold represents shared haplotype.

### *3.3. Population Structure*

To assess the variation in the population, we analyzed microsatellite loci and D-loops in AMOVA (Table 5). The $F_{ST}$ value of the microsatellite loci and D-loops were 0.025 and 0.011, respectively, indicating that there was no significant genetic differentiation between the five populations. At the same time, the results showed that the variation mainly occurred in individuals, and the interspecific difference was not significant.

**Table 5.** Analysis of molecular variance in Chinese mitten crabs (*E. sinensis*) based on microsatellite loci and D-loop sequences.

| Source of Variation | | *d.f.* | Sum of Components | Variance Components | Percentage of Variation | Fixation Index | *p*-Value |
|---|---|---|---|---|---|---|---|
| (A) Microsatellites | Among populations | 4 | 24.586 | 0.0675 | 2.48 | | |
| | Within populations | 259 | 686.342 | 2.650 | 97.52 | | |
| | Total | 263 | 710.928 | 2.718 | | 0.025 | 0.000 |
| (B) D-loop | Among groups | 1 | 0.595 | 0.021 | 4.15 | | |
| | Among populations within groups | 3 | 1.238 | −0.015 | −3.08 | | |
| | Within populations | 22 | 10.833 | 0.492 | 98.93 | | |
| | Total | 26 | 12.667 | 0.498 | | 0.011 | 0.892 |

Furthermore, this study found that *E. sinensis* have different degrees of genetic differentiation among different populations (Table 6). For the microsatellite loci, the $F_{ST}$ value ranged from near-random mating (pairwise $F_{ST}$ = 0.003 between TZ and AQ populations) to moderate differentiation (pairwise $F_{ST}$ = 0.057 between TZ and CS populations). Based on the microsatellite loci, the *Nm* ranged from 4.182 to 70.863 (Table 7). The lowest *Nm* was detected between the CS and TZ populations, and the highest between the AQ and TZ populations.

**Table 6.** Pairwise $F_{ST}$ (below diagonal) and $P$ (above diagonal) values were calculated from variations in 8 microsatellite loci and D-loop sequences among five populations of Chinese mitten crabs (*E. sinensis*).

| | Population | LH | AQ | CS | TZ | SH |
|---|---|---|---|---|---|---|
| (A) Microsatellites | LH | | 0.000 | 0.054 | 0.000 | 0.000 |
| | AQ | 0.032 | | 0.000 | 0.135 | 0.009 |
| | CS | 0.018 | 0.048 | | 0.000 | 0.000 |
| | TZ | 0.036 | 0.003 | 0.057 | | 0.793 |
| | SH | 0.036 | 0.012 | 0.056 | −0.002 | |
| (B) D-loop | LH | | 0.036 | 0.063 | 0.135 | 0.027 |
| | AQ | 0.200 | | 0.1387 | 0.928 | 0.829 |
| | CS | 0.172 | 0.021 | | 0.198 | 0.315 |
| | TZ | 0.081 | −0.030 | 0.038 | | 0.162 |
| | SH | 0.202 | −0.046 | 0.033 | 0.044 | |

Note: Pairwise $F_{ST}$ of microsatellite loci were corrected with the ENA method.

**Table 7.** *Nm* based on microsatellite loci (below diagonal) and D-loop sequences (above diagonal) between Chinese mitten crab (*E. sinensis*) populations.

| Population | LH | AQ | CS | TZ | SH |
|---|---|---|---|---|---|
| LH | | 2.000 | 2.395 | 5.678 | 1.969 |
| AQ | 7.751 | | 23.692 | inf | inf |
| CS | 13.088 | 5.022 | | 12.800 | 14.500 |
| TZ | 6.524 | 70.863 | 4.182 | | 10.989 |
| SH | 6.559 | 23.918 | 4.301 | inf | |

The STRUCTURE analysis determined K = 2 to be the most likely number of genetically distinct clusters (Figure 4A,C). This result was also reflected by the principal coordinate analysis (Figure 4B). Interestingly, the LH and CS populations were independent of the other populations. Meanwhile, the N-J tree of microsatellite loci data based on the Nei's $D_A$ genetic distance revealed that the LH population was independent, and the AQ, CS, TZ, and SH populations were clustered as one clade (Figure 5A).

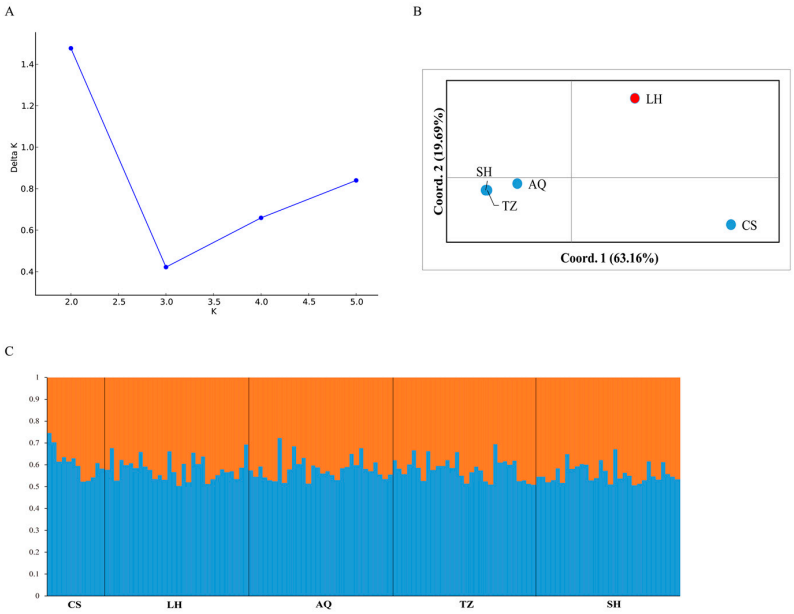


**Figure 4.** (**A**) Inference of best K based on microsatellite loci in STRUCTURE v 2.3.4. (**B**) Principal coordinate analysis (PCoA) of pairwise distances between the five populations based on microsatellite loci. (**C**) Genetic structure among Chinese mitten crab (*E. sinensis*) populations. Individual assignment to two genetically distinct clusters using STRUCTURE v 2.3.4. Likelihood of assignment for each individual is shown as a vertical bar.

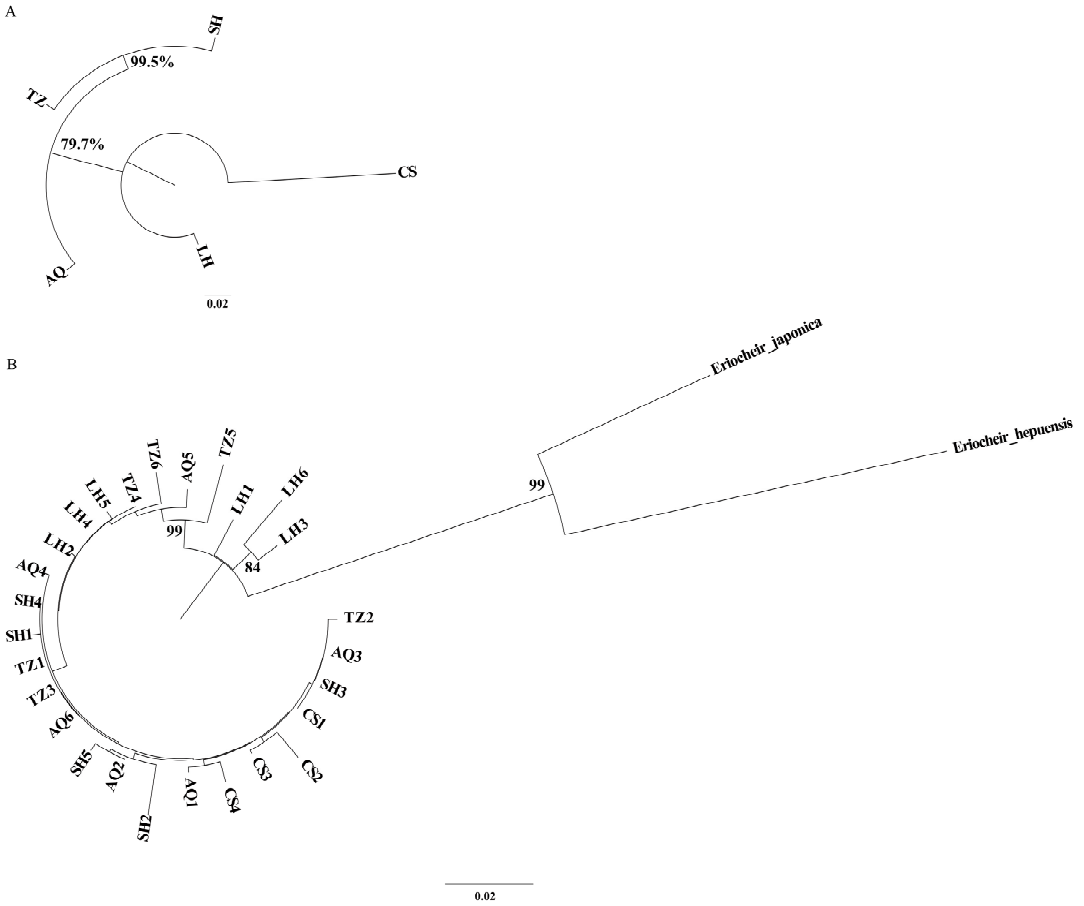


**Figure 5.** (**A**) Neighbor-joining (NJ) tree based on Nei's DA genetic distances among five populations. (**B**) Neighbor-joining (NJ) tree of all of the D-loops for Chinese mitten crabs (*E. sinensis*); letters represent populations and numbers represent individuals. The outgroups are *Eriocheir hepuensis* (FJ455506.1) and *Eriocheir japonica* (FJ455505.1).

Based on the D-loop sequences, the pairwise $F_{ST}$ ranged from 0.021 (CS and AQ populations) to 0.202 (SH and LH populations) (Table 6). In the D-loop sequence, the *Nm* ranged from 1.969 to 23.692 (Table 7). The lowest *Nm* was observed between the SH and LH populations, and the highest between the CS and AQ populations. The result of the D-loop analysis showed that in the N-J tree, half of the LH individuals clustered into one clade, while the remaining individuals were found in the Yangtze River group (Figure 5B). The haplotype network exhibited the two main branches' haplotypes, indicating that haplotypes from different regions were linked; the two shared haplotypes and dominant haplotypes were clearly defined (Figure S4A). Furthermore, the ML tree showed that haplotype 2 and haplotype 5 obtained support values of more than 80% (Figure S4B). These three haplotypes are shared haplotypes of the LH population and are consistent with the network results.

In the study, Tajima's D test and Fu's Fs test were executed on the D-loop sequences of *E. sinensis*. Both the D test value and Fs test value were negative, and they had no significant difference with 0 (Table 8), suggesting that all populations are at mutation-drift equilibrium. The mismatch distribution curve displayed a multi-peaked curve distribution, indicating a stable population size (Figure S5).

**Table 8.** Neutrality tests for D-loop sequences of Chinese mitten crabs (*E. sinensis*).

| Population | Tajima's D Test | *p*-Value | Fu's Fs Test | *p*-Value |
|---|---|---|---|---|
| LH | −0.196 | 0.435 | −1.064 | 0.154 |
| AQ | −1.011 | 0.201 | −3.709 | 0.005 |
| CS | −0.069 | 0.603 | −0.715 | 0.163 |
| TZ | −1.260 | 0.095 | −0.055 | 0.415 |
| SH | −0.526 | 0.412 | −1.716 | 0.056 |

## 4. Discussion

### *4.1. Geometric Morphological Analysis*

Geometric morphometry has proven to be an extraordinary tool for the study of morphology [10]. Morphological characters are external manifestations of intrinsic heredity and have a certain lag compared to genetic variation. Geometric morphology has the advantage of being able to exclude some confounding factors and identify morphological differences that are more difficult to detect with traditional morphology [48]. The existence of morphological differences between male and female crabs has been confirmed in a previous study [49]. Another previous study showed that differences in morphology, physiology, and even genetic levels can occur between population species due to geographical barriers [50]. In the present study, the morphology of crabs in different regional groups was found to differ slightly. The Liao River is located in northeastern China and has a cold climate, so the river crabs mature earlier and are smaller than those in the Yangtze River [51]. Our results confirm this statement. Compared with crabs from all areas of the Yangtze River, the frontal and lateral spina of female crabs in the Liao River are more closely distributed, while the M-pattern pattern of male crabs is contracted more inward. Crabs from the Liaohe River reach sexual maturity earlier than crabs from the Yangtze River. In the market, the price of mature early crabs is higher than that of crabs that mature normally. In order to improve the economic benefits of crab farming, farmers from the middle and lower reaches of the Yangtze River introduced crabs from the Liaohe River, resulting in a risk of germplasm mixture. Our results also indicated potential morphological differences among crabs in the different basins. We believe that this method has some potential for germplasm conservation by identifying crab sources and preventing germplasm mixture.

### *4.2. Genetic Diversity*

Genetic diversity represents the evolutionary flexibility of populations, and higher genetic diversity means that the population has better evolutionary potential and ability to adapt to environmental changes. Mitochondrial DNA and microsatellite loci have been widely used in the genetic analysis of crustaceans [52], such as mud crabs (*Scylla paramamosain*) [53] and swimming crabs (*Portunus trituberculatus*) [54].

At present, the genetic diversity of crab populations is unclear. Besides the occurrence of genetic mutations, crabs often copulate with multiple mates, potentially resulting in offspring more abundant in genetic diversity than their parents. In aquaculture, crabs from other basins were introduced into local farms via breeding and escaping, and the artificial breeding of crabs caused the gene exchange of populations from different basins. At present, the genetic diversity of crabs in the Yangtze River and Liaohe River has decreased, so it is urgent to maintain their genetic diversity.

Compared to the previous study, the average expected heterozygosity (0.653 to 0.678) and observed heterozygosity (0.571 to 0.712) of the studied population were lower than that of the Liaohe ($H_e$: 0.88; $H_o$: 0.79), Nanliujiang ($H_e$: 0.84; $H_o$: 0.77), and Mudanjiang ($H_e$: 0.85; $H_o$: 0.73) populations, which could be due to the different number of molecular makers, sampling number, and basins selected [55]. In addition, genetic drift is a change in allele frequency in a population, due to a random selection of certain genes. This may also account for the decline in genetic diversity. Moreover, the nucleotide diversity and haplotype diversity were important indicators of genetic diversity. The high $H_d$ (0.933 to 1) and $P_i$ (0.006 to 0.020) found in the study indicate that the populations have a high

level of diversity. As a result, although the $H_d$ and $P_i$ were both higher than critical values ($H_d$: 0.5, $P_i$: 0.05) [56], $H_d$ was higher than $P_i$ in this study, which may be due to the genetic bottleneck caused by the introduction of large crab populations from other basins [57].

### *4.3. Genetic Structure*

Genetic structure is affected by many factors, such as a change in environment, climate change, and ecological structural changes [22]. Using nuclear and mitochondrial genetic markers may provide a more comprehensive explanation of genetic conditions [54,58–60]. The pairwise $F_{ST}$ of the Liaohe River and Yangtze River crabs in this study was higher than in other studies [55,61], and we found a high *Nm* (all population > 1), indicating that there is gene flow between the Yangtze River and Liaohe River populations. The gene flow model is mainly classified into the island model (continent island model and island model), the stepping stone model, and the isolation by distance model [62,63]. The island model is suitable for populations with discontinuous habitats. The geographical distance between the Yangtze River and the Liao River is far (more than 985 km), which is consistent with the island pattern. These two basins have a strong geographical barrier, and the existence of gene exchange may be caused by aquaculture activity practices or the displacement of crabs as wild germplasm. Crabs from the Liaohe River basin were introduced to the Yangtze River basin for farming, and it is speculated that the farmed Liaohe population escaped and therefore had a gene exchange with the wild population in the Yangtze River basin [1].

An earlier study using microsatellite loci analysis showed that the Yangtze River and Liaohe River crabs share the same ancestry, and different gene pools exist due to biological evolution and natural geographic isolation [3]. In the present study, as seen from the results of the AMOVA analysis, the genetic differentiation between populations was not obvious (microsatellite: 2.48%; D-loop: 1.07%), and the genetic variation was mainly within populations (microsatellite: 97.52%; D-loop: 98.93%). This indicates that the genetic exchange between the Yangtze River and Liaohe River populations is frequent and genetic exchange is constant. Interestingly, within the Yangtze population, the microsatellite loci results showed that the CS population was clearly different from the other Yangtze populations, and the pairwise $F_{ST}$ of the CS and TZ populations (0.056), and that of the CS and SH populations (0.055) was higher than 0.05, meaning they have moderate genetic differentiation [61]. A previous study found that the crabs from the same basin failed to cluster together, suggesting that the genetic differentiation of populations may not be related to geographic distance [1,64]. The sample size had a significant impact on the data analysis [65], and we speculate that the small number of crabs from the CS population was one of the reasons. In addition, it is possible that some crabs were collected earlier than those at other sites, and the crab collection site was close to the shore, meaning there might have been an escape from the farmed population [66,67]. However, in the D-loop sequence results, the pairwise $F_{ST}$ within the Yangtze populations were all less than 0.05, and the genetic differentiation was not obvious. It is possible that the mutation rates of the two molecular makers are different, resulting in inconsistent genetic signals [22,61].

Tajima's D test, Fu's Fs test, and mismatched distribution were important indices in the analysis of the historical evolution of the population [20]. The negative results of both Tajima's D and Fu's Fs tests, as well as the multi-peaked results of the mismatched distribution curve, indicate that there was no population expansion in the recent past [68,69].

## 5. Conclusions

In conclusion, this study accurately distinguished wild *E. sinensis* from different basins by geometric morphometry. The genetic diversity of wild *E. sinensis* in the Yangtze River and the Liaohe River is relatively high, and there is moderate to strong gene flow between the populations in the two basins. These results suggest a risk of genetic homogeneity in *E. sinensis* populations from different basins. Thus, it is very important to take timely measures to strengthen the protection of the germplasm resources of *E. sinensis*. This

study elucidates the genetic resources of wild Chinese mitten crabs (*E. sinensis*) and lays a foundation for the conservation and development of their germplasm resources.

**Supplementary Materials:** The following supporting information can be downloaded at: https://www.mdpi.com/article/10.3390/fishes8050253/s1, Table S1: Morphometric information of Chinese mitten crab (*E. sinensis*) populations; Table S2: Primers information of Chinese mitten crab (*E. sinensis*) populations in the present study; Table S3: Relative contribution of each landmark of four populations in Chinese mitten crab (*E. sinensis*); Table S4: Eigenvalues and contributions of the first ten principal components of relative warps scores; The discriminatory formula; Figure S1. Landmark points for morphological measurements on the carapace of Chinese mitten crab (*E. sinensis*); Figure S2. (A) Mean shape of landmarks on carapace of wild Chinese mitten crab (*E. sinensis*) from different populations. (B) superimposed landmarks of Chinese mitten crab (*E. sinensis*) of four population; Figure S3. (A)The variance of Principal components; (B) Scatter plots of PC1 and PC2 of wild Chinese mitten crab (*E. sinensis*) from different basins; (C) The change of 30 landmarks of PC1; (D) The change of 30 landmarks of PC2; Figure S4. (A) The median-joining network based on haplotype frequencies of Chinese mitten crab (*E. sinensis*). (B) Maximum likelihood tree based on haplotypes from D-loop region sequences; Figure S5. Mismatch distribution for the five inferred populations of Chinese mitten crab (*E. sinensis)*.

**Author Contributions:** L.Z. collected the crab samples, performed the experiment, analyzed the data, and wrote the manuscript. J.G. analyzed the data and assisted in writing and proofreading the article. Y.Y. collected the crab samples. Z.N. provided language help. K.L. provided the study materials, laboratory animals, and instruments. G.X. and J.G. conceptualized the experiment. All authors have read and agreed to the published version of the manuscript.

**Funding:** This work was supported by the Central Public-interest Scientific Institution Basal Research Fund, Freshwater Fisheries Research Center, CAFS (NO. 2021JBFM06), and the earmarked fund for CARS48.

**Institutional Review Board Statement:** Institutional Animal Care and Use Committee of the Ministry of Freshwater Fisheries Research Center, Chinese Academy of Fishery Sciences. (SYXK(HX)20210104006).

**Data Availability Statement:** The datasets generated and/or analyzed for the current study are available from the corresponding author on reasonable request.

**Acknowledgments:** The authors would like to express their sincere thanks to the personnel of these teams for their kind assistance.

**Conflicts of Interest:** The authors declare no conflict of interest.

## References

1. Sui, L.; Zhang, F.; Wang, X.; Bossier, P.; Sorgeloos, P.; Hänfling, B. Genetic Diversity and Population Structure of the Chinese Mitten Crab *Eriocheir sinensis* in Its Native Range. *Mar. Biol.* **2009**, *156*, 1573–1583. (In Chinese) [CrossRef]
2. Wang, H.; Feng, G.; Zhang, Y. Studies on Genetic Diversity of Chinese Mitten Crab *Eriocheir sinensis* of Yangtze River System Based on Mitochondrial DNA Control Region. *J. Phys. Conf. Ser.* **2020**, *1549*, 032010. [CrossRef]
3. Chang, Y.; Liang, L.; Ma, H.; He, J.; Sun, X. Microsatellite Analysis of Genetic Diversity and Population Structure of Chinese Mitten Crab (*Eriocheir sinensis*). *J. Genet. Genom.* **2008**, *35*, 171–176. [CrossRef] [PubMed]
4. Wang, J.; Xu, P.; Zhou, G.; Li, X.; Lu, Q.; Liu, X.; Zhou, J.; Wang, C. Genetic Improvement and Breeding Practices for Chinese Mitten Crab, *Eriocheir sinensis*. *J. World Aquac. Soc.* **2018**, *49*, 292–301. [CrossRef]
5. Deng, Y.; Xu, Y.; Xu, Z.; Yang, Y.; Bai, R.; Ge, J.; Pan, J. Progress in Genetic Breeding of Chinese Mitten Crab. *J. Aquac.* **2017**, *38*, 39–42. (In Chinese)
6. Li, J.; Chen, H.; Geng, X.; Dong, X.; Sun, J. Genetic Diversity Analysis of Wild and Cultured Population of *Eriocheir sinensis* from Different Water Systems. *Prog. Fish. Sci.* **2019**, *40*, 105–113. (In Chinese) [CrossRef]
7. Espinoza-Donoso, S.; Angulo-Bedoya, M.; Lemic, D.; Benítez, H.A. Assessing the Influence of Allometry on Sexual and Non-Sexual Traits: An Example in *Cicindelidia trifasciata* (Coleoptera: Cicindelinae) Using Geometric Morphometrics. *Zool. Anz.* **2020**, *287*, 61–66. [CrossRef]
8. Benítez, H.A.; Briones, R.; Jerez, V. Intra and Inter-Population Morphological Variation of Shape and Size of the Chilean Magnificent Beetle, Ceroglossus Chilensis in the Baker River Basin, Chilean Patagonia. *J. Insect Sci.* **2011**, *11*, 1536–2442. [CrossRef]
9. Kaliontzopoulou, A.; Carretero, M.A.; Llorente, G.A. Intraspecific Ecomorphological Variation: Linear and Geometric Morphometrics Reveal Habitat-Related Patterns within *Podarcis bocagei* Wall Lizards. *J. Evol. Biol.* **2010**, *23*, 1234–1244. [CrossRef]

10. Tozetto, L.; Lattke, J.E. Revealing Male Genital Morphology in the Giant Ant Genus Dinoponera with Geometric Morphometrics. *Arthropod Struct. Dev.* **2020**, *57*, 100943. [CrossRef]
11. dos Santos, C.F.; Souza dos Santos, P.D.; Marques, D.M.; da-Costa, T.; Blochtein, B. Geometric Morphometrics of the Forewing Shape and Size Discriminate *Plebeia* Species (Hymenoptera: Apidae) Nesting in Different Substrates. *Syst. Entomol.* **2019**, *44*, 787–796. [CrossRef]
12. Trallero, L.; Farré, M.; Phillips, R.A.; Navarro, J. Geometric Morphometrics Reveal Interspecific and Sexual Differences in Bill Morphology in Four Sympatric Planktivorous Petrels. *J. Zool.* **2019**, *307*, 167–177. [CrossRef]
13. Walker, J.A. Ecological Morphology of Lacustrine Threespine *Stickleback Gasterosteus Aculeatus* L. (Gasterosteidae) Body Shape. *Biol. J. Linn. Soc.* **1997**, *61*, 3–50. [CrossRef]
14. Ponton, D.; Carassou, L.; Raillard, S.; Borsa, P. Geometric Morphometrics as a Tool for Identifying *Emperor fish* (Lethrinidae) Larvae and Juveniles. *J. Fish Biol.* **2013**, *83*, 14–27. [CrossRef]
15. Gemilang Simanjuntak, R.; Eprilurahman, R.; Selatan, M.J.T.; Utara, S.; Yogyakarta, I. Geometric Morphometrics Analysis of Chelae and Carapace of the Freshwater Prawn Macrobrachium Bate, 1868. *Biog. J. Ilm. Biol.* **2019**, *7*, 58–66. [CrossRef]
16. Torres, M.V.; Giri, F.; Collins, P.A. Geometric Morphometric Analysis of the Freshwater Prawn *Macrobrachium borellii* (Decapoda: Palaemonidae) at a Microgeographical Scale in a Floodplain System. *Ecol. Res.* **2014**, *29*, 959–968. [CrossRef]
17. Zheng, C.; Jiang, T.; Luo, R.; Chen, X.; Liu, H.; Yang, J. Geometric Morphometric Analysis of the Chinese Mitten Crab *Eriocheir sinensis*: A Potential Approach for Geographical Origin Authentication. *N. Am. J. Fish. Manag.* **2021**, *41*, 891–903. [CrossRef]
18. Brian, J.V.; Fernandes, T.; Ladle, R.J.; Todd, P.A. Patterns of Morphological and Genetic Variability in UK Populations of the Shore Crab, *Carcinus maenas* Linnaeus, 1758 (Crustacea: Decapoda: *Brachyura*). *J. Exp. Mar. Bio. Ecol.* **2006**, *329*, 47–54. [CrossRef]
19. Binashikhbubkr, K.; Adam Malik, A.; Al-Misned, F.; Mahboob, S.; Naim, D.M. Geometric Morphometric Discrimination between Seven Populations of Kawakawa Euthynnus Affinis (Cantor, 1849) from Peninsular Malaysia. *J. King Saud Univ.-Sci.* **2022**, *34*, 101863. [CrossRef]
20. Grover, A.; Sharma, P.C. Development and Use of Molecular Markers: Past and Present. *Crit. Rev. Biotechnol.* **2016**, *36*, 290–302. [CrossRef]
21. Zhang, W.; Jiang, S.; Salumy, K.R.; Xuan, Z.; Xiong, Y.; Jin, S.; Gong, Y.; Wu, Y.; Qiao, H.; Fu, H. Comparison of Genetic Diversity and Population Structure of Eight *Macrobrachium nipponense* Populations in China Based on D-Loop Sequences. *Aquac. Rep.* **2022**, *23*, 101086. [CrossRef]
22. Sun, N.; Zhu, D.M.; Li, Q.; Wang, G.Y.; Chen, J.; Zheng, F.; Li, P.; Sun, Y.H. Genetic Diversity Analysis of *Topmouth culter* (Culter Alburnus) Based on Microsatellites and D-Loop Sequences. *Environ. Biol. Fishes* **2021**, *104*, 213–228. [CrossRef]
23. Gallagher, J.; Finarelli, J.A.; Jonasson, J.P.; Carlsson, J. Mitochondrial D-Loop DNA Analyses of Norway Lobster (Nephrops Norvegicus) Reveals Genetic Isolation between Atlantic and East Mediterranean Populations. *J. Mar. Biol. Assoc. UK* **2019**, *99*, 933–940. [CrossRef]
24. Duan, B.; Liu, W.; Li, S.; Yu, Y.; Guan, Y.; Mu, S.; Li, Z.; Ji, X.; Kang, X. Microsatellite Analysis of Genetic Diversity in Wild and Cultivated *Portunus trituberculatus* in Bohai Bay. *Mol. Biol. Rep.* **2022**, *49*, 2543–2551. [CrossRef]
25. Guo, X.Z.; Chen, H.M.; Wang, A.B.; Qian, X.Q. Population Genetic Structure of the Yellow Catfish (*Pelteobagrus fulvidraco*) in China Inferred from Microsatellite Analyses: Implications for Fisheries Management and Breeding. *J. World Aquac. Soc.* **2022**, *53*, 174–191. [CrossRef]
26. Vieira, M.L.C.; Santini, L.; Diniz, A.L.; de Freitas Munhoz, C. Microsatellite Markers: What They Mean and Why They Are so Useful. *Genet. Mol. Biol.* **2016**, *39*, 312–328. [CrossRef]
27. Wirgin, I.; Maceda, L.; Stabile, J.; Waldman, J. Genetic Population Structure of Summer Flounder Paralichthys Dentatus Using Microsatellite DNA Analysis. *Fish. Res.* **2022**, *250*, 106270. [CrossRef]
28. Wang, Y.J.; Lu, J.H.; Liu, Z.; Zhang, J.P. Genetic Diversity of *Gymnocypris chilianensis* (Cypriniformes, Cyprinidae) Unveiled by the Mitochondrial DNA D-Loop Region. *Mitochondrial. DNA Part B Resour.* **2021**, *6*, 1292–1297. [CrossRef]
29. Hansen, M.M.; Kenchington, E.; Nielsen, E.E. Assigning Individual Fish to Populations Using Microsatellite DNA Markers. *Fish Fish.* **2001**, *2*, 93–112. [CrossRef]
30. Ma, H.; Ma, C.; Ma, L.; Cui, H. Novel Polymorphic Microsatellite Markers in *Scylla paramamosain* and Cross-Species Amplification in Related Crab Species. *J. Crustac. Biol.* **2010**, *30*, 441–444. [CrossRef]
31. Liu, Y.G.; Guo, Y.H.; Hao, J.; Liu, L.X. Genetic Diversity of Swimming Crab (*Portunus trituberculatus*) Populations from Shandong Peninsula as Assessed by Microsatellite Markers. *Biochem. Syst. Ecol.* **2012**, *41*, 91–97. [CrossRef]
32. Švara, V.; Norf, H.; Luckenbach, T.; Brack, W.; Michalski, S.G. Isolation and Characterization of Eleven Novel Microsatellite Markers for Fine-Scale Population Genetic Analyses of Gammarus Pulex (Crustacea: Amphipoda). *Mol. Biol. Rep.* **2019**, *46*, 6609–6615. [CrossRef]
33. González-Castellano, I.; González-López, J.; González-Tizón, A.M.; Martínez-Lage, A. Genetic Diversity and Population Structure of the Rockpool Shrimp Palaemon Elegans Based on Microsatellites: Evidence for a Cryptic Species and Differentiation across the Atlantic–Mediterranean Transition. *Sci. Rep.* **2020**, *10*, 10784. [CrossRef] [PubMed]
34. Su, Y.; Zhang, C.; Li, Q.; Zheng, H.; Cheng, Y.; Wu, X. Genetic Diversity Analysis of Wild and Cultured *Eriocheir sinensis* Populations from the Yangtze River, Yellow River, and Liaohe River Based on the Mitochondrial D-Loop Gene. *J. Fish. Sci. China* **2019**, *26*, 436–444. (In Chinese) [CrossRef]

35. Xiao, Q. DNA Molecular Markers Discovery of Chinese Mitten Crab *Eriocheir sinensis* and Its Application. Master's Thesis, Shanghai Ocean University, Shanghai, China, 2018. (In Chinese).
36. Klingenberg, C.P. MorphoJ: An Integrated Software Package for Geometric Morphometrics. *Mol. Ecol. Resour.* **2011**, *11*, 353–357. [CrossRef]
37. IBM SPSS. *Corp Ibm SPSS Statistics for Windows, Version 26.0*; IBM Corp: Armonk, NY, USA, 2018.
38. Thompson, J.D.; Gibson, T.J.; Higgins, D.G. Multiple Sequence Alignment Using ClustalW and ClustalX. *Curr. Protoc. Bioinform.* **2003**, *Chapter 2*, 1–22. [CrossRef]
39. Librado, P.; Rozas, J. DnaSP v5: A Software for Comprehensive Analysis of DNA Polymorphism Data. *Bioinform. Appl. Note* **2009**, *25*, 1451–1452. [CrossRef]
40. Excoffier, L.; Lischer, H.E.L. Arlequin Suite Ver 3.5: A New Series of Programs to Perform Population Genetics Analyses under Linux and Windows. *Mol. Ecol. Resour.* **2010**, *10*, 564–567. [CrossRef]
41. Van Oosterhout, C.; Hutchinson, W.F.; Wills, D.P.M.; Shipley, P. MICRO-CHECKER: Software for Identifying and Correcting Genotyping Errors in Microsatellite Data. *Mol. Ecol. Notes* **2004**, *4*, 535–538. [CrossRef]
42. Goudet, J. FSTAT (Version 2.9.3.2): A Program to Estimate and Test Gene Diversities and Fixation Indices. Available online: http//www.unil.ch/izea/software/fstat.html (accessed on 22 June 2022).
43. Evanno, G.; Regnaut, S.; Goudet, J. Detecting the Number of Clusters of Individuals Using the Software Structure: A Simulation Study. *Mol. Ecol.* **2005**, *14*, 2611–2620. [CrossRef]
44. Pritchard, J.K. Documentation for Structure Software: Version 2.2. *J. Pediatr. Surg.* **2009**, *41*, 55–63.
45. Baum, B.R. PHYLIP: Phylogeny Inference Package. Version 3.2. Joel Felsenstein. *Q. Rev. Biol.* **1989**, *64*, 539–541. [CrossRef]
46. Peakall, R.; Smouse, P.E. GENALEX 6: Genetic Analysis in Excel. Population Genetic Software for Teaching and Research. *Mol. Ecol. Notes* **2006**, *6*, 288–295. [CrossRef]
47. Peakall, R.; Smouse, P.E. GenALEx 6.5: Genetic Analysis in Excel. Population Genetic Software for Teaching and Research-an Update. *Bioinformatics* **2012**, *28*, 2537–2539. [CrossRef] [PubMed]
48. Jiang, X.; Cheng, Y.; Pan, J.; Li, X.; Wu, X. Landmark-Based Morphometric Identification of Wild *Eriocheir sinensis* with Geographically Different Origins. *J. Fish. Sci. China* **2019**, *26*, 1116–1125. (In Chinese)
49. Lu, Y.; Wu, X.; He, J.; Wang, C.; Li, X.; Liu, N.; Wang, Y.; Cheng, Y. Comparative Studies of the Morphology and Biochemical Composition of Wild Juvenile Chinese Mitten Crabs from the Yangtze River, Yellow River and Liaohe River Systems. *J. Fish. Sci. China* **2016**, *23*, 382–395. (In Chinese)
50. Li, Y.; Li, S.; Wang, C.; Li, C.; Zhao, J. Establishment and Application of Morphological Discrimination Model for Juveniles *Eriocheir sinensis* from Liaohe, Yangtze and Oujiang Rivers. *J. Fish. China* **2001**, *25*, 120–126. (In Chinese)
51. Zu, L.; Yu, Q.; Jiang, X.; Cheng, Y.; Wu, X. Edible Yield and Proximate Composition Analysis of Wild Male Adult Mitten Crab, *Eriocheir* Sp. in Northern China. *Fish. Sci.* **2021**, *40*, 20–28.
52. Zhang, W.; Lv, J.; Ti, X.; Zhao, X.Y.; Jin, L.; Wu, J.; Gao, B.; Liu, P. Verification of an Efficient Genetic Sex Identification Method in *Portunus trituberculatus*: Applied to Study Sex Ratios in Full-Sib Families. *Aquaculture* **2021**, *543*, 736976. [CrossRef]
53. Wang, W.; Ma, C.; Chen, W.; Jin, Z.; Zhao, M.; Zhang, F.; Liu, Z.; Ma, L. Population Genetic Diversity of Mud Crab (*Scylla paramamosain*) from Southeast Coastal Regions of China Based on Mitochondrial COI Gene Sequence. *Gene* **2020**, *751*, 144763. [CrossRef]
54. Duan, B.; Mu, S.; Guan, Y.; Li, S.; Yu, Y.; Liu, W.; Li, Z.; Ji, X.; Kang, X. Genetic Diversity and Population Structure of the Swimming Crab (*Portunus trituberculatus*) in China Seas Determined by Genotyping-by-Sequencing (GBS). *Aquaculture* **2022**, *555*, 738233. [CrossRef]
55. Wang, S.; Luo, L.; Zhang, R.; Guo, K.; Xu, W.; Zhao, Z. Population Genetic Diversity and Differentiation of Mitten Crab, Genus Eriocheir, Based on Microsatellite Markers. *Fishes* **2022**, *7*, 182. (In Chinese) [CrossRef]
56. Grant, W.S.; Bowen, B.W. Shallow Population Histories in Deep Evolutionary Lineages of Marine Fishes: Insights from Sardines and Anchovies and Lessons for Conservation. *J. Hered.* **1998**, *89*, 415–426. [CrossRef]
57. Qiu, G.; Xu, Q.; Wang, L.; Fan, Z.; Chen, X. Molecular Taxonomy and Phylogeny of Four Species of Eriocheir (Decapoda: Brachyura: Grapsidae). *Acta Zool. Sin.* **2001**, *47*, 640–647.
58. Raabová, J.; Münzbergová, Z.; Fischer, M. Ecological Rather than Geographic or Genetic Distance Affects Local Adaptation of the Rare Perennial Herb, Aster Amellus. *Biol. Conserv.* **2007**, *139*, 348–357. [CrossRef]
59. Xu, J.; Chu, K.H. Genome Scan of the Mitten Crab Eriocheir Sensu Stricto in East Asia: Population Differentiation, Hybridization and Adaptive Speciation. *Mol. Phylogenet. Evol.* **2012**, *64*, 118–129. [CrossRef]
60. Guo, E.; Cui, Z.; Wu, D.; Hui, M.; Liu, Y.; Wang, H. Genetic Structure and Diversity of Portunus Trituberculatus in Chinese Population Revealed by Microsatellite Markers. *Biochem. Syst. Ecol.* **2013**, *50*, 313–321. [CrossRef]
61. Wright, S. The Interpretation of Population Structure by F-Statistics with Special Regard to Systems of Mating. *Evolution* **1965**, *19*, 395–420. [CrossRef]
62. Marko, P.B.; Hart, M.W. The Complex Analytical Landscape of Gene Flow Inference. *Trends Ecol. Evol.* **2011**, *26*, 448–456. [CrossRef]
63. Hey, J. Recent Advances in Assessing Gene Flow between Diverging Populations and Species. *Curr. Opin. Genet. Dev.* **2006**, *16*, 592–596. [CrossRef]

64. Chen, W.; Li, C.; Chen, F.; Li, Y.; Yang, J.; Li, J.; Li, X. Phylogeographic Analyses of a Migratory Freshwater Fish (*Megalobrama terminalis*) Reveal a Shallow Genetic Structure and Pronounced Effects of Sea-Level Changes. *Gene* **2020**, *737*, 144478. [CrossRef] [PubMed]
65. Bao, W.; Shu, J.; Xu, S.; Li, H.; Chen, G. Effects of Sample Size and Sex Ratio on Various Genetic Diversity Measures with Microsatellite Markers. *Genet. Breed.* **2007**, *43*, 6–9. (In Chinese)
66. Xiao, Q.; Liu, Q.; Wu, X.; Wang, H.; Dong, P.; Liu, H.; Cheng, Y. Genetic Diversity Analysis of Wild and Cultured Megalopa Population of *Eriocheir sinensis* from Yangtze River. *Genom. Appl. Biol.* **2017**, *36*, 1935–1945. (In Chinese) [CrossRef]
67. Fraser, D.J.; Cook, A.M.; Eddington, J.D.; Bentzen, P.; Hutchings, J.A. Mixed Evidence for Reduced Local Adaptation in Wild Salmon Resulting from Interbreeding with Escaped Farmed Salmon: Complexities in Hybrid Fitness. *Evol. Appl.* **2008**, *1*, 501–512. [CrossRef]
68. Gu, Q.; Wu, H.; Zhou, C.; Cao, X.; Wang, W.; Wen, Y.; Luo, F. Genetic Structure and Phylogeographic Relationships of the Bellamya Complex: A Nascent Aquacultural Snail in the Pearl River Basin, China. *Aquac. Res.* **2020**, *51*, 1323–1335. [CrossRef]
69. Frandsen, H.R.; Figueroa, D.F.; George, J.A. Mitochondrial Genomes and Genetic Structure of the Kemp's Ridley Sea Turtle (*Lepidochelys kempii*). *Ecol. Evol.* **2020**, *10*, 249–262. [CrossRef]